J. Chem. Sci. Vol. 124, No. 6, November 2012, pp. 1353–1364.

μ-Phenoxo-μ-pseudohalide and μ-pseudohalide dinuclear, tetranuclear and one-dimensional complexes: magneto-structural correlation and interesting type of solid state isomerism

SUJIT SASMAL and SASANKASEKHAR MOHANTA*

Department of Chemistry, University of Calcutta, 92, A P C Road, Kolkata 700 009, India
e-mail: sm_cu_chem@yahoo.co.in

Abstract. Five Schiff base ligands have been utilized to explore metallo-pseudohalide (azide or cyanate) systems. These ligands are the 1:1 condensation products of 3-methoxysalicylaldehyde with ethanolamine (H_2L^1)/1-(2-aminoethyl)-piperidine (HL^2)/ 4-(2-aminoethyl)-morpholine (HL^3) or salicylaldehyde with 1-(2-aminoethyl)-piperidine (HL^4)/4-(2-aminoethyl)-morpholine (HL^5). The derived complexes are as follows: Four heterobridged μ-phenoxo-$\mu_{1,1}$-azide/cyanate dinickel(II) compounds of composition $[Ni^{II}_2(HL^1)_3(\mu_{1,1}\text{-}N_3)]\cdot 3H_2O$ (**1**), $[Ni^{II}_2(L^2)_2(\mu_{1,1}\text{-}N_3)(N_3)(H_2O)]\cdot CH_3CH_2OH$ (**2**), $[Ni^{II}_2(L^3)_2(\mu_{1,1}\text{-}N_3)(CH_3CN)(H_2O)](ClO_4)\cdot H_2O\cdot CH_3CN$ (**3**) and $[Ni^{II}_2(HL^1)_3(\mu_{1,1}\text{-}NCO)]\cdot 2H_2O$ (**4**); Two $\mu_{1,3}$-azide bridged tetranickel(II) compounds $[\{Ni^{II}(L^4)(\mu_{1,3}\text{-}N_3)(H_2O)\}_4]$ (**5**) and $[\{Ni^{II}(L^5)(\mu_{1,3}\text{-}N_3)(H_2O)\}_4]$ (**6**); Two $\mu_{1,3}$-azide/cyanate one-dimensional compounds $[Cu^{II}L^5(\mu_{1,3}\text{-}NCO)]_n\cdot 2nH_2O$ (**7**) and $[Cu^{II}L^5(\mu_{1,3}\text{-}N_3)]_n\cdot 2nH_2O$ (**8**). Except compound **5** which shows overall antiferromagnetic coupling, other compounds exhibit overall ferromagnetic interaction. Syntheses, crystal structures, magnetic properties, density functional theoretical (DFT) calculations and experimental/theoretical magneto-structural correlations have been carried out which have revealed some interesting observations on composition/topology, magneto-structural correlations and solid state isomerism. The results have been already published. The present report deals with a review of the salient and interesting features of these works.

Keywords. Metallo-pseudohalides; magneto-structural correlations; DFT; heterobridged.

1. Introduction

Molecular magnetism is a frontier research area.[1–5] One major focus in this area is to determine magneto-structural correlations, both experimental and theoretical.[1–4] In an experimental correlation, J versus one parameter (for example, bridge angle) relationship is determined for a few similar complexes. However, it is not possible to keep other governing parameters constant for these complexes, which may be considered as a limitation of experimental magneto-structural correlations. Therefore, it deserves importance if at least a pair of similar exchange-coupled systems are obtained for which all but one governing parameters are identical. On the other hand, at least for symmetrically bridged compounds, it is easily possible to change one governing parameter keeping others constant theoretically in the model systems and thus the effect of the change of other parameters is nullified in the theoretical correlations in symmetrically bridged systems. However, it is difficult to avoid the above mentioned limitation even in the theoretical correlations of heterobridged systems (for example, μ-phenoxo-$\mu_{1,1}$-azide dinuclear complexes) because it is not possible to change one parameter keeping all others constant (for example, the change of metal-phenoxo-metal angle is associated with change of metal-phenoxo distance in μ-phenoxo-$\mu_{1,1}$-azide dinuclear complexes). Thus, determination of even the theoretical magneto-structural correlations in heterobridged systems deserves importance in molecular magnetism.

The research in structural chemistry focusing supramolecular chemistry/crystal engineering is another area which is being attracted vast fascination in recent years because of two major objectives of the self-assemblies: aesthetic beauty and possibility of being functional materials.[6] Another perspective of solid state structural chemistry is to explore the little investigated types of isomerism as well as to find out new types of isomerism. Regarding non-classical types of isomerism that have been developed in recent years, the following may be mentioned as examples: Jahn–Teller isomerism,[7] supramolecular isomerism,[8] molecular isomerism due to difference in number of interstitial solvent molecules,[9] catenation isomerism.[10]

*For correspondence

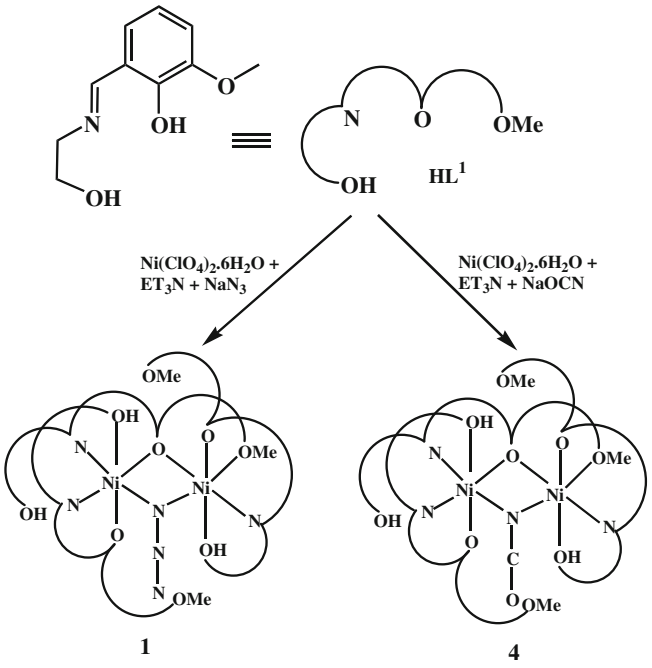

Scheme 1. Syntheses of **1** and **4**.

Metallo-pseudohalide, azide or cyanate, species have been always of great interest in molecular magnetism and supramolecular chemistry/crystal engineering due to a number of coordination modes of these potentially bridging ligands as well as due to their ability to mediate ferro or antiferromagnetic interactions among metal centres. The most usual bridging modes are the end-on ($\mu_{1,1}$-, commonly expressed as EO)[1a,1d,11–17] and end-to-end ($\mu_{1,3}$-, EE),[1a,1d,18,19] but some others like, $\mu_{1,1,1}$-,[13,16,20,21] $\mu_{1,1,3}$-,[14,21] $\mu_{1,1,1,1}$-,[22] and $\mu_{1,1,3,3}$-[23] have been also described. This way, a number of azide/cyanate-bridged systems of different nuclearity (dinuclear, oligonuclear and polynuclear clusters) and also of 1D, 2D, and 3D topologies have been achieved and there is a considerable amount of information available on experimental and theoretical magneto-structural correlations.[1a,1d,11–23]

Despite all the encouraging results, it is difficult to control the composition/topology of the metallo-pseudohalide species, which depends on factors like organic ligand, metal ion, solvent, stoichiometric ratio of reactants and other reaction conditions. To explore the metallo-pseudohalide species, we have

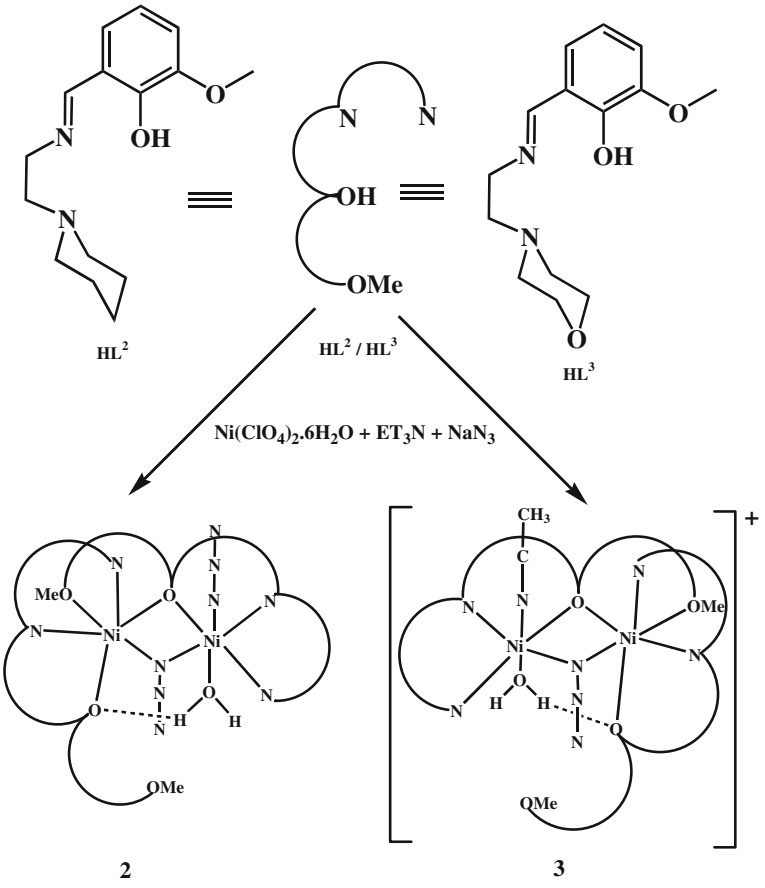

Scheme 2. Syntheses of **2** and **3**.

used five Schiff base ligands H_2L^1, HL^2, HL^3, HL^4 and HL^5, which are the [1+1] condensation products of 3-methoxysalicylaldehyde with ethanolamine (for H_2L^1) / 1-(2-aminoethyl)-piperidine (for HL^2) / 4-(2-aminoethyl)-morpholine (for HL^3) or of salicylaldehyde with 1-(2-aminoethyl)-piperidine (for HL^4) / 4-(2-aminoethyl)-morpholine (for HL^5). We have synthesized the following compounds using these ligands: Four heterobridged μ-phenoxo-$\mu_{1,1}$-azide/cyanate dinickel(II) compounds of composition $[Ni^{II}_2(HL^1)_3(\mu_{1,1}\text{-}N_3)]\cdot 3H_2O$ (**1**), $[Ni^{II}_2(L^2)_2(\mu_{1,1}\text{-}N_3)(N_3)(H_2O)]\cdot CH_3CH_2OH$ (**2**), $[Ni^{II}_2(L^3)_2(\mu_{1,1}\text{-}N_3)(CH_3CN)(H_2O)](ClO_4)\cdot H_2O\cdot CH_3CN$ (**3**) and $[Ni^{II}_2(HL^1)_3(\mu_{1,1}\text{-}NCO)]\cdot 2H_2O$ (**4**); Two single end-to-end azide bridged cyclic tetranickel(II) clusters of composition $[\{Ni^{II}(L^4)(\mu_{1,3}\text{-}N_3)(H_2O)\}_4]$ (**5**) and $[\{Ni^{II}(L^5)(\mu_{1,3}\text{-}N_3)(H_2O)\}_4]$ (**6**); Two single end-to-end azide/cyanate bridged one-dimensional copper(II) systems of composition $[Cu^{II}L^5(\mu_{1,3}\text{-}NCO)]_n\cdot 2nH_2O$ (**7**), $[Cu^{II}L^5(\mu_{1,3}\text{-}N_3)]_n\cdot 2nH_2O$ (**8**). Single crystal X-ray structure determination and variable-temperature/field magnetic studies have been done for all these eight

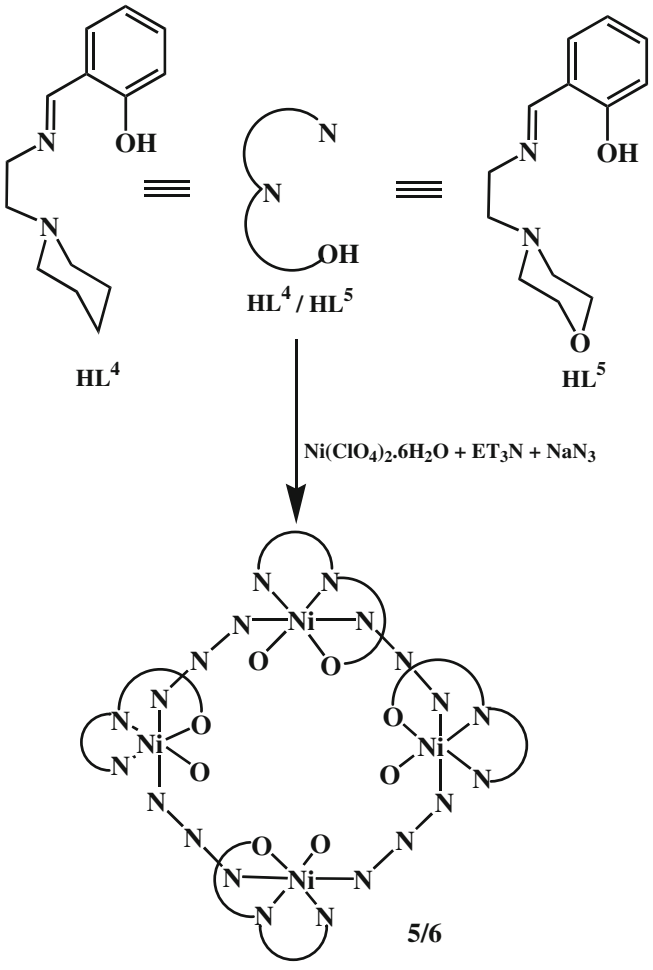

Scheme 3. Syntheses of **5** and **6**.

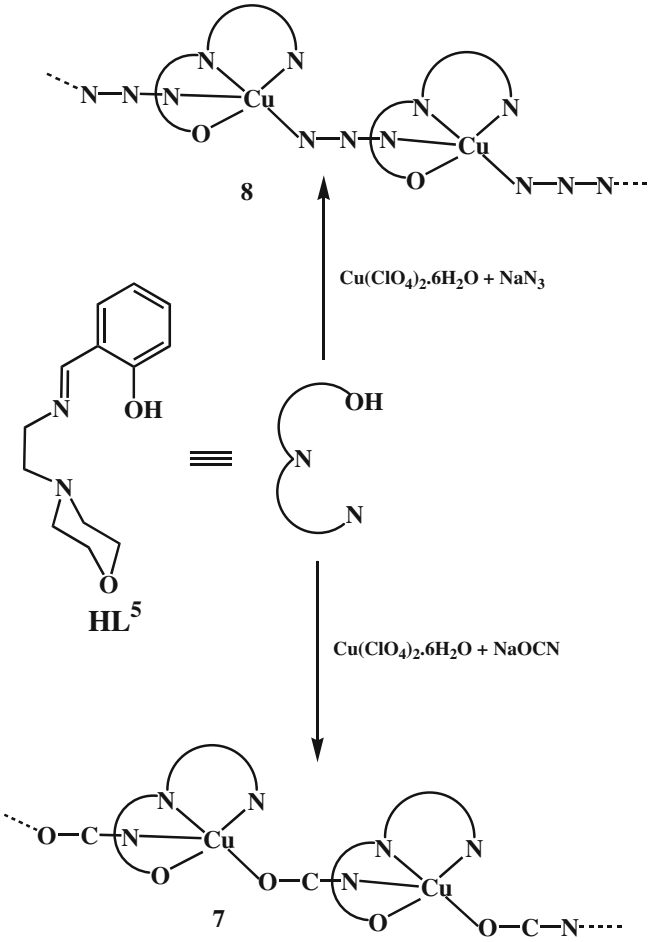

Scheme 4. Syntheses of **7** and **8**.

compounds. Density functional theoretical calculations on magnetic properties have been carried out for **1**–**3**, **5** and **6**. Interesting experimental and theoretical magneto-structural correlations have been determined and new types of isomerism have been observed. The results have been already published.[24–28] A review of the salient features of these works is being presented here.

2. Outline of syntheses

The dinickel(II) or tetranickel(II) complexes **1**–**6** are readily obtained in high yield from the reaction of the corresponding Schiff base ligand H_2L^1/HL^2/HL^3/HL^4/HL^5, nickel(II) perchlorate hexahydrate, triethylamine and sodium azide/cyanate in 3:2:6:2 ratio (for **1** and **4**) or in 1:1:1:4 ratio (for **2**, **3**, **5** and **6**). For the copper(II) systems **7** and **8**, the Schiff base: copper(II) perchlorate hexahydrate: sodium azide/cyanate ratio of 1:1:4 was used; the use of the base triethylamine was not required in these cases. The syntheses of the eight compounds are demonstrated in schemes 1, 2, 3 and 4.

3. Crystal structures, and magneto-structural correlations of heterobridged μ-phenoxo-$\mu_{1,1}$-azide/cyanate dinickel(II) compounds: Combined experimental and theoretical exploration[24–26]

Crystal structures of $Ni^{II}_2(HL^1)_3(\mu_{1,1}\text{-}N_3)]\cdot 3H_2O$ (**1**) and $[Ni^{II}_2(L^2)_2(\mu_{1,1}\text{-}N_3)(N_3)(H_2O)]\cdot CH_3CH_2OH$ (**2**) are shown in figures 1 and 2, while the crystal structures of $[Ni^{II}_2(L^3)_2(\mu_{1,1}\text{-}N_3)(CH_3CN)(H_2O)](ClO_4)\cdot H_2O\cdot CH_3CN$ (**3**) and $[Ni^{II}_2(HL^1)_3(\mu_{1,1}\text{-}NCO)]\cdot 2H_2O$ (**4**) are shown in figures S1 and S2 (supplementary informations). The structures reveal that **1**–**3** are μ-phenoxo-$\mu_{1,1}$-azide dinickel(II) compounds, while **4** is a μ-phenoxo-$\mu_{1,1}$-cyanate dinickel(II) compound.

The azide analogue **1** and the cyanate analogue **4** are derived from the same ligand and have similar type of structures containing three monodeprotonated ligands, $[HL^1]^-$, in which the phenoxo moiety is deprotonated. Among the three phenolate oxygen atoms of three $[HL^1]^-$, one bridges the two metal ions, while each of the remaining two is coordinated to each of the two metal ions in monodentate fashion. Of the three alcohol oxygen atoms, one is uncoordinated, while each of the other two coordinates to each of the two metal ions in monodentate fashion. Among the three imine nitrogen atoms, two are coordinated to one metal ion, while the third coordinates to the second metal centre. Of the three ethereal oxygen atoms, one is coordinated to one metal ion, while the other two remain uncoordinated. In addition to the phenoxo bridge, the two metal centres are also bridged by the nitrogen atom of an end-on azide (in **1**) or cyanate (in **4**) ligand.

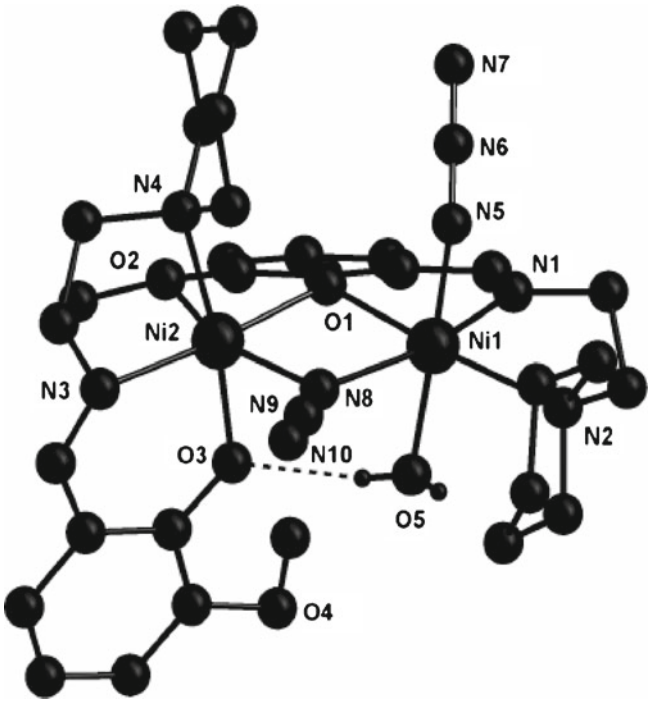

Figure 2. Crystal structure of $[Ni^{II}_2(L^2)_2(\mu_{1,1}\text{-}N_3)(N_3)(H_2O)]\cdot CH_3CH_2OH$ (**2**). Hydrogen atoms, except those of water molecule, and solvated ethanol molecule are omitted for clarity.[26,30]

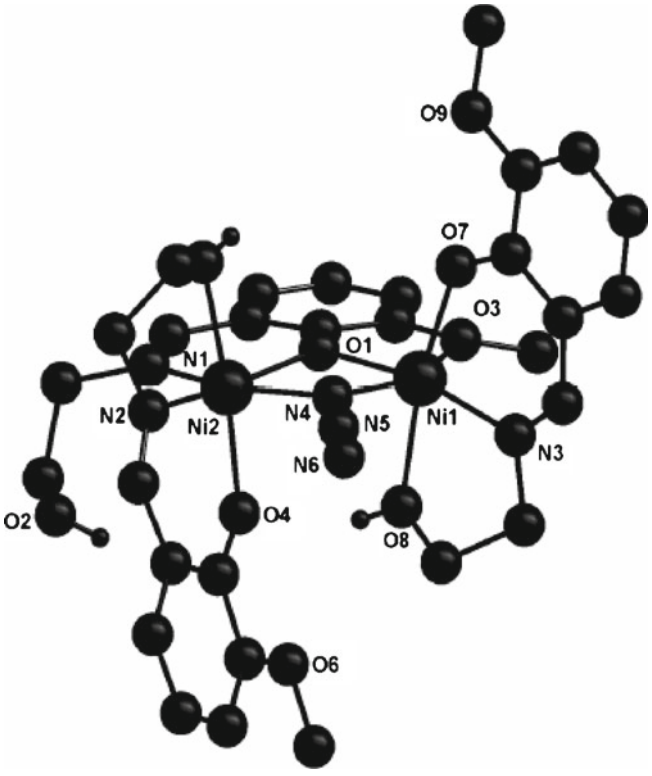

Figure 1. Crystal structure of $[Ni^{II}_2(HL^1)_3(\mu_{1,1}\text{-}N_3)]\cdot 3H_2O$ (**1**). Hydrogen atoms, except of three alcohol moieties, and three water molecules are deleted for clarity.[24,29]

Compounds **2** and **3** contain two deprotonated ligands, $[L^2]^-/[L^3]^-$. While one of the two phenoxo oxygen atoms of two $[L^2]^-/[L^3]^-$ bridges the two metal ions, the second phenoxo oxygen atom coordinates one metal ion. The two metal ions are additionally bridged by the nitrogen atom of an end-on azide ligand. Among the two methoxy oxygen atoms of two $[L^2]^-/[L^3]^-$, one is non-coordinated, while the second is coordinated to one metal centre. Each of the two metal ions are coordinated also to the imine and piperidine (for **2**)/morpholine (for **3**) nitrogen atoms of each of the two $[L^2]^-/[L^3]^-$.

Magnetic properties of the heterobridged μ-phenoxo-$\mu_{1,1}$-azide/cyanate dinickel(II) compounds **1**–**4** are shown in figures 3, 4, supplementary figures S3 and S4, respectively, as $\chi_M T$ versus T plots. The profiles indicate that the metal centres in all the four compounds are ferromagnetically coupled. Using the Hamiltonian $\mathbf{H} = -2J(\mathbf{S_1}\cdot\mathbf{S_2}) + D_1\left[S^2_{Z,1}\right] + D_2\left[S^2_{Z,2}\right]$, good

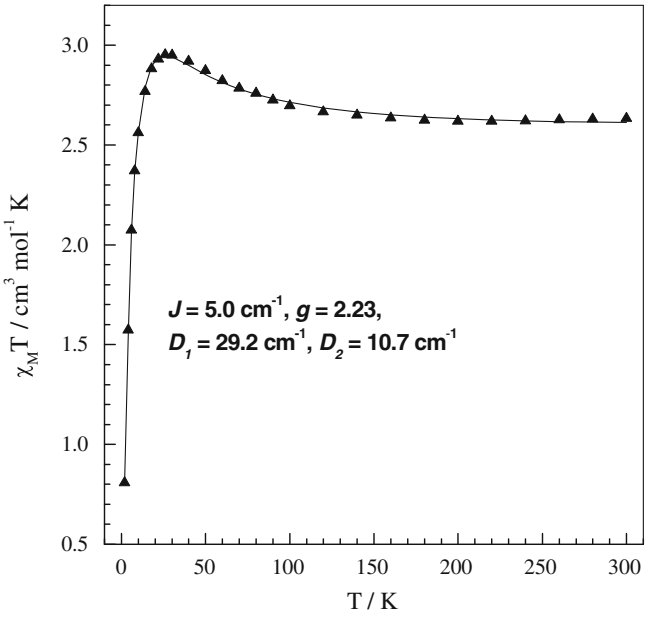

Figure 3. $\chi_M T$ vs. T plots for $[Ni_2^{II}(HL^1)_3(\mu_{1,1}\text{-}N_3)]\cdot 3H_2O$ (**1**). Symbols and solid lines represent the observed and calculated data, respectively.[24,29]

quality simulations are obtained (figures 3, 4, supplementary figures S3 and S4) with following parameters: $J = 5.0\,cm^{-1}$, $g = 2.23$, $D_1 = 29.2\,cm^{-1}$ and $D_2 = 10.7\,cm^{-1}$ for **1**; $J = 16.6\,cm^{-1}$, $g = 2.2$ and $D_1 = D_2 = -7.3\,cm^{-1}$ for **2**; $J = 16.92\,cm^{-1}$, $g = 2.2$ and $D_1 = D_2 = -6.41\,cm^{-1}$ for **3**; $J = 3.33\,cm^{-1}$, $g = 2.24$ and $D_1 = D_2 = |6.68|\,cm^{-1}$ for **4**.

Both the phenoxo and azide routes are responsible for the superexchange between the metal centres in a heterobridged μ-phenoxo-$\mu_{1,1}$-azide compound, such as **1**–**3**. So, the nickel–azide–nickel and nickel–phenoxo–nickel angles and two nickel–azide and two nickel–phenoxo distances should be the governing factors for the J values in these compounds. Magnetic and structural parameters of the **1**–**3** and also of the only two previously reported μ-phenoxo-$\mu_{1,1}$-azide dinickel(II) compounds are summarized in table 1.

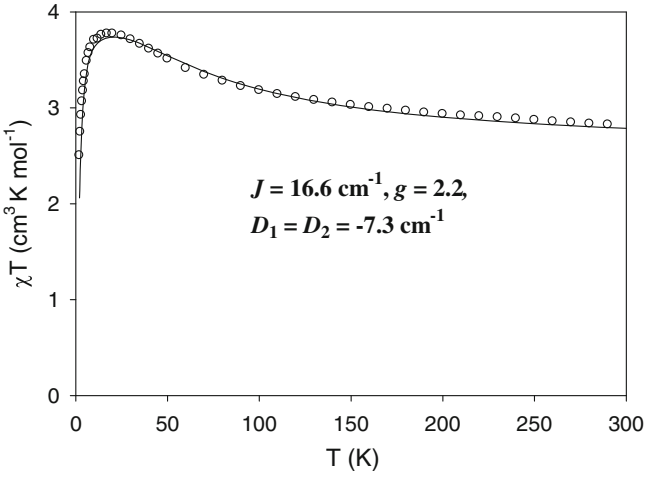

Figure 4. $\chi_M T$ vs. T plots for $[Ni_2^{II}(L^2)_2(\mu_{1,1}\text{-}N_3)(N_3)(H_2O)]\cdot CH_3CH_2OH$ (**2**). Symbols and solid lines represent the observed and calculated data, respectively.[26,30]

For the two compounds **1** and **IA** (table 1),[31a] J values are drastically different; $5.0\,cm^{-1}$ for **1** and $25.6\,cm^{-1}$ for **IA**. Of the four governing parameters, the nickel–azide–nickel and nickel–phenoxo–nickel angles and both the nickel–phenoxo distances are practically identical for these two compounds. Only the nickel–azide bond distances are different; 2.09 and 2.21 Å for **1** and 2.13 and 2.15 Å for **IA**. Clearly, the significant difference in the J values arises due to difference in nickel–azide bridge distances. Thus, interestingly, these two compounds represent a unique pair for which all but one governing parameters are identical and also represent a unique pair demonstrating the bridge distance dependency of exchange integral. The asymmetry (0.12 Å in **1**, 0.02 Å in **IA**) in the two nickel–azide bond distances are greater in **1** than in **IA**. Thus, it seems that more the asymmetry in the two nickel–azide bond distances less the strength of ferromagnetic interaction. Such J versus asymmetry correlation is also valid for compound **2** (table 1; $J = 16.6\,cm^{-1}$, asymmetry = 0.06 Å), although other governing parameters of **2** are not identical with those of **1** or **IA** and thus the J versus asymmetry correlation can be considered as more strengthened. On the other hand, the J and asymmetry of compounds **3** and **IB**[31b] are not in line with this correlation. So, it seems that although asymmetry in the two nickel–azide bond distances has some profound roles, the overall interaction is a composite effect of several parameters. Therefore, we have performed density functional theoretical calculations on the magnetic properties of **1**–**3** and **IA**. We have also determined theoretical magneto-structural correlations to get more insight regarding the role of the possible governing parameters, including asymmetry in the two nickel–azide bond distances.

Broken symmetry density functional calculations[32] of exchange interaction provide good numerical estimate of J values compared to experiments (table 1). Taking compound **2** as the model system, we have developed three different correlations. As mentioned in introduction section, the presence of dissimilar bridges prevents variation of only one structural parameter at a time to develop correlations. Therefore, we have defined three parameters (α, β and γ) to vary two parameters (angles as well as the Ni–O or Ni–N

Table 1. Magnetic and structural parameters of the five μ-phenoxo-$\mu_{1,1}$-azide dinickel(II) compounds.[26,30]

Compounds	$J_{Expt.}$ (cm^{-1})	J_{DFT} (cm^{-1})	Ni–O–Ni (°)	Ni–N–Ni (°)	Ni–O (Å)	Average Ni–O (Å)	Asymmetry in Ni–O (Å)	Ni–N (Å)	Average Ni–N (Å)	Asymmetry in Ni–N (Å)	Ref.
1	5.0	14.1	106.9	96.3	1.99, 1.99	1.99	0.00	2.09, 2.21	2.15	0.12	24
2	16.6	15.8	103.0	98.0	2.01, 2.06	2.035	0.05	2.08, 2.14	2.11	0.06	26
3	16.9	15.35	104.7	97.0	1.99, 2.02	2.005	0.03	2.12, 2.11	2.115	0.01	26
IA	25.6	18.5	106.7	96.5	1.98, 1.99	1.985	0.01	2.13, 2.15	2.14	0.02	31a
IB	2.85	12.65/10.05	102.3	95.6	2.00, 2.04	2.02	0.04	2.11, 2.14	2.125	0.03	31b

distances) at a time in our correlations. To underpin the role of asymmetry on the bond lengths, the asymmetry present in the bond distances were maintained same throughout.

$\alpha = \frac{Ni-O-Ni}{d(avg.Ni-O)}$	$\beta = \frac{Ni-N-Ni}{d(avg.Ni-N)}$	$\gamma = \frac{Ni-N-Ni}{d(Ni_B-N)}$

According to the J versus α correlation (figure S5), the magnitude of ferromagnetic J is decreased with the increase of the Ni–O–Ni angle or the decrease of the Ni–O distance. As shown in figure S6, the J versus β correlation indicates that the ferromagnetic interaction is increased as the nickel–azide–nickel angle increases or nickel–azide distance decreases, with a maximum at $\beta = 106°$. The J versus γ correlation (figure 5) reveals that ferromagnetic J is increased with the increase of γ to reach saturation at very large γ values. To understand the dependency of J on the asymmetry (Δ) in two nickel–azide distances, which is our major goal, the change in the Ni–N–Ni angle in the J versus γ correlation is ignored to get a J versus asymmetry profile, as plotted in figure 6. The asymmetry values in this graph are both positive and negative with reference to the fixed Ni_A–N distance of 2.082 Å. The asymmetry is negative when $d_{NiB-N} > 2.082$ Å, while a positive asymmetry means $d_{NiB-N} < 2.082$ Å. Although the shape of the curve in both the positive and negative asymmetry regions is closely linear, the role of asymmetry differs; while increase in negative asymmetry decreases the ferromagnetic interaction, increase in positive asymmetry increases the ferromagnetic interaction, albeit this saturates at larger value. As evident from this plot, if the Ni_B–N distance is larger than 2.082 Å (i.e., if the asymmetry is negative), an increase in asymmetry will lead

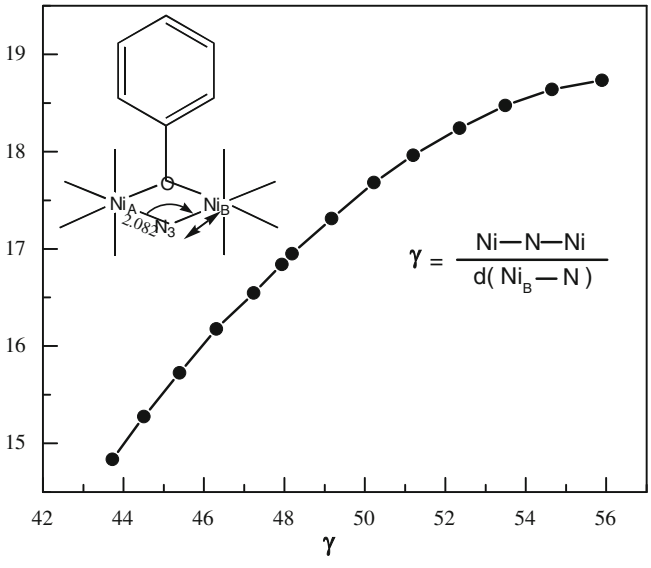

Figure 5. DFT-computed J versus γ correlation.[26,30]

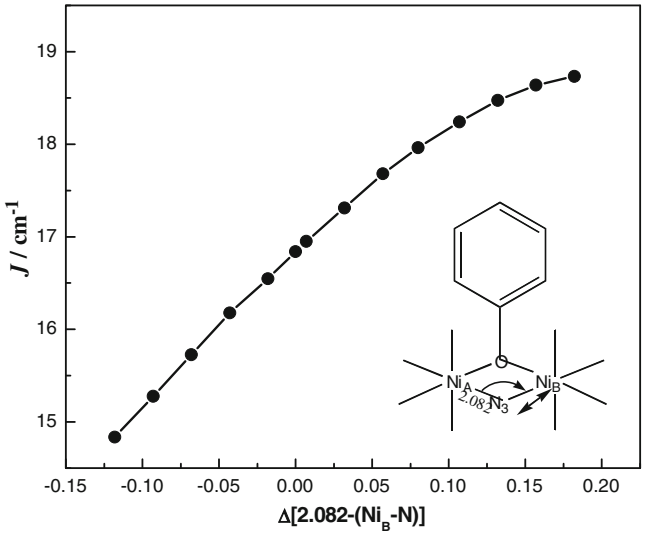

Figure 6. DFT-computed J versus asymmetry in the two Ni–N distances correlation (the variation in the Ni–N–Ni angle is ignored).[26,30]

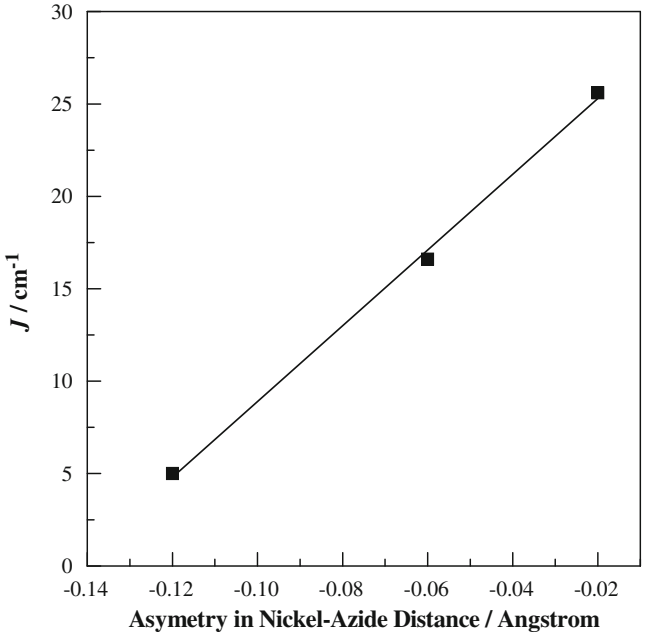

Figure 7. Linear magneto-structural correlation between experimental J and asymmetry in two nickel-azide distances.[26,30]

to a smaller ferromagnetic J and vice versa. In fact, such a trend (where Δ = shorter Ni–N bond distance – longer Ni–N bond distance) has been observed experimentally in **1** (Δ is -0.12 Å and $J = 5.0$ cm^{-1}), **2** (Δ is -0.06 Å and $J = 16.6$ cm^{-1}) and **IA** (Δ is -0.02 Å and $J = 25.6$ cm^{-1}); the linear magneto-structural correlation, on the basis of the experimental data of **1**, **2** and **IA**, between exchange integral and asymmetry is shown in figure 7. Thus, asymmetry in the two nickel–azide bond distances has been established both experimentally and theoretically as a major factor to govern the extent of ferromagnetic interaction in heterobridged μ-phenoxo-$\mu_{1,1}$-azide dinickel(II) compounds.

4. Crystal structures and magneto-structural correlation studies and theoretical calculations of a unique family of single end-to-end azide bridged Ni_4^{II} cyclic clusters[27]

The crystal structures of $[\{Ni^{II}(L^4)(\mu_{1,3}\text{-}N_3)(H_2O)\}_4]$ (**5**) and $[\{Ni^{II}(L^5)(\mu_{1,3}\text{-}N_3)(H_2O)\}_4]$ (**6**) are shown in figures 8 and 9. Overall, the structures of both species **5** and **6** can be described in a similar way; where all Ni^{II} centres within each molecule are hexacoordinated and bounded to $[L^4]^-$ or $[L^5]^-$ through the phenoxo oxygen, imine and piperidine/morpholine nitrogen atoms of the corresponding ligand. The remaining coordination sites are satisfied by one molecule of H_2O and two nitrogen atoms from N_3^- anions. The latest act as bridges between Ni^{II} ions and eventually, only four azido groups are linked to the same number of Ni^{II} centres resulting in the formation of cyclic $[Ni_4^{II}]$ systems. Interestingly, compounds **5** and **6** are the sole examples of tetranuclear clusters generated exclusively by end-to-end azide bridging ligands to date.

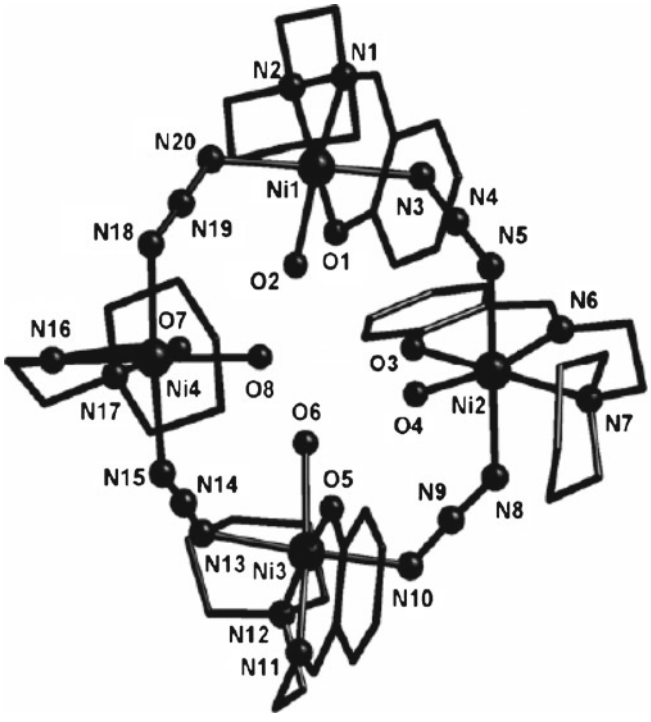

Figure 8. Crystal structure of $[\{Ni^{II}(L^4)(\mu_{1,3}\text{-}N_3)(H_2O)\}_4]$ (**5**). All the hydrogen atoms are omitted for clarity.[27,33]

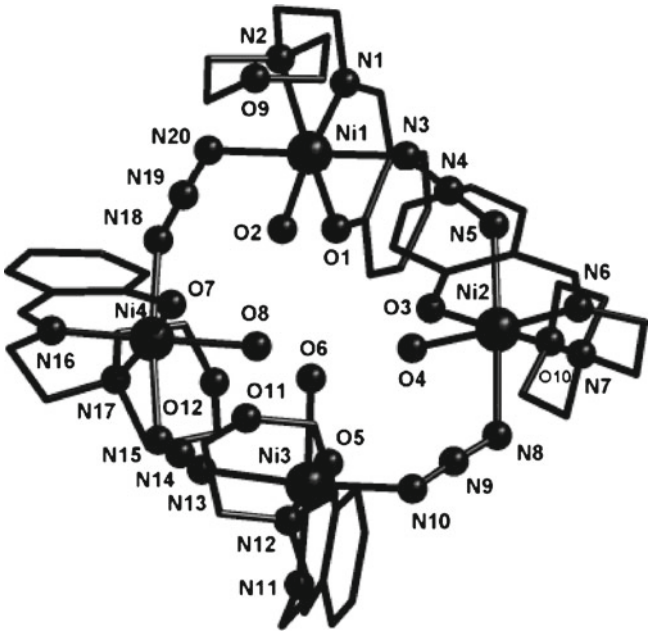

Figure 9. Crystal structure of [{$Ni^{II}(L^5)(\mu_{1,3}\text{-}N_3)(H_2O)$}$_4$] (**6**). All the hydrogen atoms are omitted for clarity.[27,33]

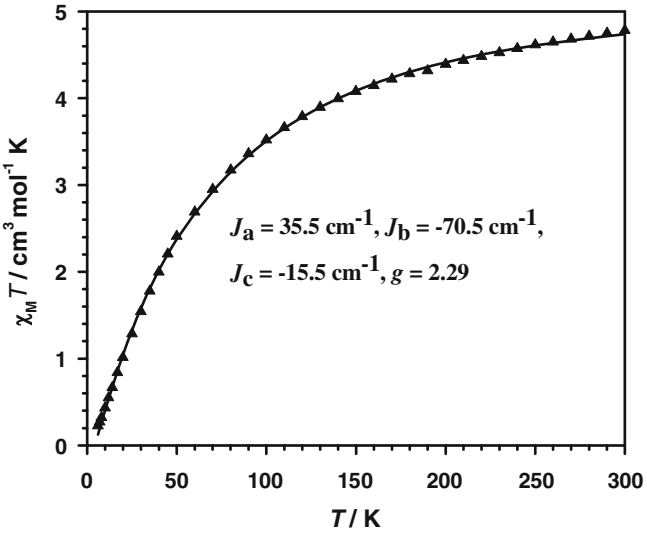

Figure 10. Observed (symbols) and calculated (solid lines) $\chi_M T$ versus T plots for [{$Ni^{II}(L^4)(\mu_{1,3}\text{-}N_3)(H_2O)$}$_4$] (**5**).[27,33]

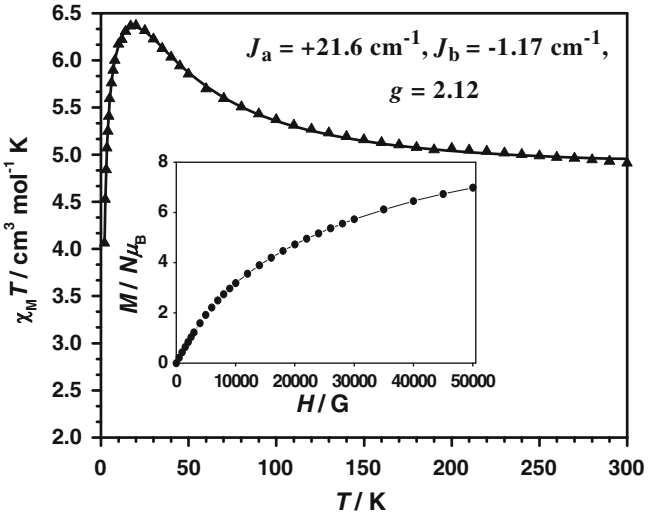

Figure 11. Observed (symbols) and calculated (solid lines) $\chi_M T$ versus T plots for [{$Ni^{II}(L^5)(\mu_{1,3}\text{-}N_3)(H_2O)$}$_4$] (**6**). The inset is an isothermal $M/N\mu_B$ vs. H/G plot at 2.0 K.[27,33]

The magnetic data of **5** and **6** are shown in figures 10 and 11 as $\chi_M T$ versus T plots. It is interesting that the magnetic behaviour of the two complexes is drastically different; Interaction is antiferromagnetic in one, **5**, but ferromagnetic in the second, **6**. For the end-to-end azide bridged systems, two key parameters which govern the magnetic properties are Ni–N–N angles and Ni–N$\cdots$N–Ni torsion angles, τ.[1,18,19] Between these two, the Ni–N–N angles range almost similarly in the two complexes and so the difference in magnetic properties is expected to originate from the difference in the τ values: three types in **5** (87.5/90.6°, 50.4° and 3.3°) but two types in **6** (85.4/86.1° and 54.7/57.8°). It is known that the interaction should be antiferromagnetic if τ is 0° and the antiferromagnetism decreases as τ increases from 0° to 90°. Hence, compound **5** has an overall moderate antiferromagnetic behaviour due to the presence of an exchange pathway with an unprecedented Ni–N$\cdots$N–Ni torsion angle (3.3°) close to 0°, while complex **6** exhibits a predominant ferromagnetic behaviour because the torsion angles in this case lie in between *ca*. 50° and 90°.

Depending on the types of the τ values, the magnetic data of **5** were modelled/fitted with three-J Hamiltonian $\mathbf{H} = -2J_a(\mathbf{S_1}\cdot\mathbf{S_2} + \mathbf{S_3}\cdot\mathbf{S_4}) - 2J_b(\mathbf{S_2}\cdot\mathbf{S_3}) - 2J_c(\mathbf{S_4}\cdot\mathbf{S_1})$, while the two-$J$ Hamiltonian $\mathbf{H} = -2J_a(\mathbf{S_1}\cdot\mathbf{S_2} + \mathbf{S_3}\cdot\mathbf{S_4}) - 2J_b(\mathbf{S_2}\cdot\mathbf{S_3} + \mathbf{S_4}\cdot\mathbf{S_1})$ are used for **6**. The converging fitting parameters are listed in table 2. Importantly, $J = -35.25$ cm^{-1} corresponding to $\tau = 3.3°$ and is responsible for antiferromagnetism in **5**.

To model the magnetic properties theoretically, density functional theoretical calculations[36] have been performed on **5** and **6** with the four-J Hamiltonian $\mathbf{H} = -2J_{12}(\mathbf{S_1}\cdot\mathbf{S_2}) - 2J_{23}(\mathbf{S_2}\cdot\mathbf{S_3}) - 2J_{34}(\mathbf{S_3}\cdot\mathbf{S_4}) - 2J_{41}(\mathbf{S_4}\cdot\mathbf{S_1})$. The theoretical J values are compared with the experimental values in table 2; the trend is nicely matched. Interestingly, DFT-computed J values reproduce the trend of the $\chi_M T$ versus T profile nicely (figure S7), indicating the ability of DFT methods in reproducing exchange Integrals.

Table 2. Torsion angles and experimental and density functional theoretical J values for single end-to-end azide bridged tetranickel(II) compounds **5** and **6**.

Ni–N···N–Ni torsion angle (°)	J (DFT)/ cm^{-1}		J (Expt)/ cm^{-1}	
Antiferromagnetic compound [{$Ni^{II}(L^4)(\mu_{1,3}$-$N_3)(H_2O)$}$_4$] (**5**)				
90.6	+7.45	J_{12}	+17.75	J_a
3.3	−42.65	J_{23}	−35.25	J_b
87.5	+8.55	J_{34}	+17.75	J_a
50.4	−9.3	J_{41}	−7.75	J_c
Ferromagnetic compound [{$Ni^{II}(L^5)(\mu_{1,3}$-$N_3)(H_2O)$}$_4$] (**6**)				
85.4	+7.05	J_{12}	+10.8	J_a
54.7	−2.25	J_{23}	−0.58	J_b
86.1	+7.75	J_{34}	+10.8	J_a
57.8	−0.6	J_{41}	−0.58	J_b

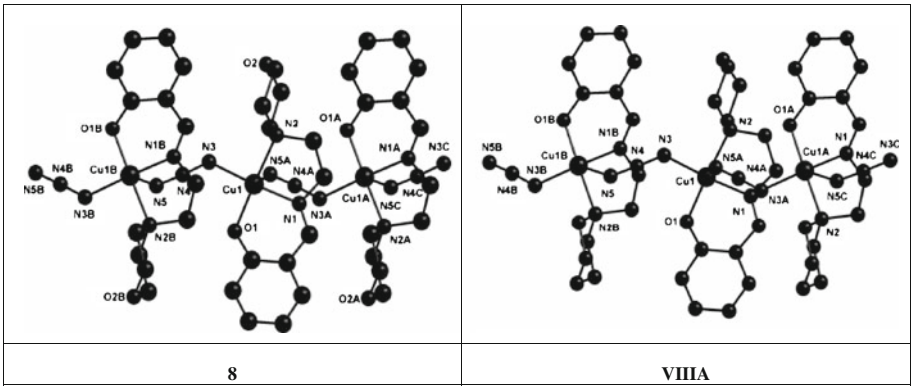

Figure 12. Crystal structures of $[Cu^{II}L^5(\mu_{1,3}$-$N_3)]_n \cdot 2nH_2O$ (**8**) and $[Cu^{II}L^5(\mu_{1,3}$-$N_3)]_n \cdot 2nH_2O$ (**VIIIA**). Hydrogen atoms and water molecules are not shown for clarity. Symmetry codes for **8**: A, −x, −0.5+y, 0.5–z; B, −x, 0.5+y, 0.5–z ; C, x, −1+y, z. Symmetry codes for **VIIIA**: A, 2–x, 0.5+y, 0.5–z ; B, 2–x, −0.5+y, 0.5–z ; C, x, y–1, z.[28,34,35]

5. Crystal structures and magnetic properties of two one-dimensional end-to-end azide/cyanate bridged copper(II) compounds: new type of solid state isomerism[28]

The perspective views of the end-to-end azide/cyanate bridged one-dimensional copper(II) systems $[Cu^{II}L^5(\mu_{1,3}$-NCO)$]_n \cdot 2nH_2O$ (**7**) and $[Cu^{II}L^5(\mu_{1,3}$-$N_3)]_n \cdot 2nH_2O$ (**8**) are shown in figures S8 and S12, respectively. While the phenoxo oxygen atom and imine and morpholine nitrogen atoms of one deprotonated ligand, $[L^5]^-$, satisfy the three coordination positions, the remaining two coordination positions of the pentacoordinated and distorted square pyramidal metal centre are satisfied by two nitrogen atoms of two end-to-end bridging azide ligands for **8** and by one nitrogen atom and one oxygen atom of two end-to-end bridging cyanate ligands for **7**.

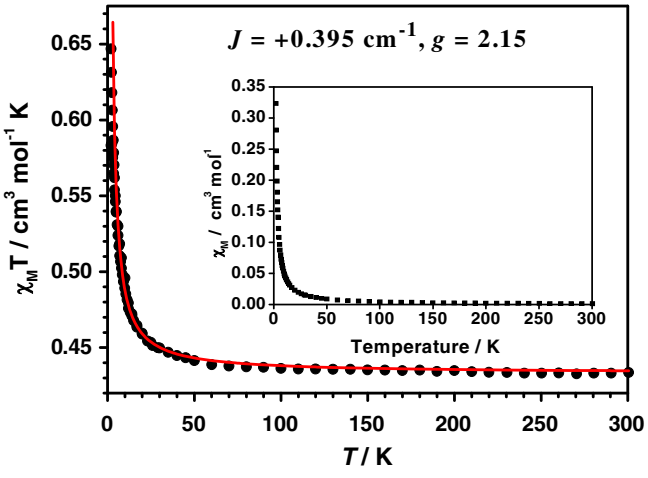

Figure 13. Fittings of the $\chi_M T$ vs. T of $[Cu^{II}L^5(\mu_{1,3}$-$N_3)]_n \cdot 2nH_2O$ (**8**) between 2.0 and 300.0 K. The experimental data is shown as squares and the solid lines correspond to the theoretical values. Inset shows χ_M vs. T data.[28,35]

Table 3. Comparison of the crystallographic data of $[Cu^{II}L^5(\mu_{1,3}\text{-}N_3)]_n{\cdot}2nH_2O$ (**8**) and $[Cu^{II}L^5(\mu_{1,3}\text{-}N_3)]_n{\cdot}2nH_2O$ (**VIIIA**).

	8	**VIIIA**
Formula	$C_{13}H_{17}N_5O_4Cu$ [a]	$C_{13}H_{21}N_5O_4Cu$ [a]
Formula weight	370.86 [a]	374.90 [a]
Crystal colour	Blue	Blue
Crystal system	Monoclinic	Monoclinic
Space group	$P2_1/c$	$P2_1/c$
a, Å	9.4934(15)	9.497(6)
b, Å	9.2962(14)	9.410(2)
c, Å	18.377(3)	18.232(8)
V, Å^3	1606.4(4)	1604.5(13)
α, °	90.00	90.00
β, °	97.902(2)	100.01(3)
γ, °	90.00	90.00
Z	4	4

[a]Four water hydrogen atoms in **8** were not located. Actual formula and formula weight are same for both.

The magnetic data of **7** and **8** are shown in figure S9 and figure 13,[28,35] respectively, as $\chi_M T$ versus T plots. The profiles indicate the existence of ferromagnetic interaction in both the compounds. The magnetic data were fitted/modelled with the Hamiltonian $\mathbf{H} = -2J\Sigma\mathbf{SA_i}{\cdot}\mathbf{SA_{i+1}}$.[1a,37] As shown by the solid lines in figure S9 and figure 13, good quality fitting has been obtained with $J = +0.095\,cm^{-1}$ and $g = 2.13$ for the cyanate analogue **7** and $J = +0.395\,cm^{-1}$ and $g = 2.15$ for the azide analogue **8**. It may be mentioned that compound **7** is the sole example of ferromagnetically coupled EE cyanate bridged 1-D copper(II) system.

Synthesis, crystal structure and magnetic properties of a compound $[Cu^{II}L^5(\mu_{1,3}\text{-}N_3)]_n{\cdot}2nH_2O$ (**VIIIA**) have been reported previously.[34] Compound $[Cu^{II}L^5(\mu_{1,3}\text{-}N_3)]_n{\cdot}2nH_2O$ (**8**) and $[Cu^{II}L^5(\mu_{1,3}\text{-}N_3)]_n{\cdot}2nH_2O$ (**VIIIA**) are derived from the same ligand (HL^5) and both have same composition. The azide-bridged one-dimensional topology of both **8** and **VIIIA** are also same (figure 12). So, it may seem that **8** and **VIIIA** is the same compound. However, interestingly, the magnetic behaviour of **8** and **VIIIA** are drastically different; **8** exhibits ferromagnetic interaction with $J = +0.395\,cm^{-1}$, while **VIIIA** exhibits antiferromagnetic interaction with $J = -2.15\ cm^{-1}$. Thus, on the basis of the drastic difference in magnetic properties, it is clear that **8** and **VIIIA** is not the same compound but they are magnetic isomers. Interestingly, such type of magnetic isomerism is unprecedented. Now, comparison of the crystallographic data in table 3 reveals another interesting and unprecedented aspect: except β, other parameters are practically identical, revealing that this pair represents another new type of solid state isomerism which may be called crystallographic isomerism. Again, comparison of the structural parameters (table S1) indicates that some parameters are identical, while some others are different. On the basis of these similarities-dissimilarities of the structural parameters, the pair can also be called crystallographic isomerism. Now, let us look into the position of the two solvated water molecule in figure 14, revealing that positions of the water molecule are different. Moreover, the number/types of hydrogen bonds and overall supramolecular structures are also different; **8** is three-dimensional (figures S10 and S11), while **VIIIA** is

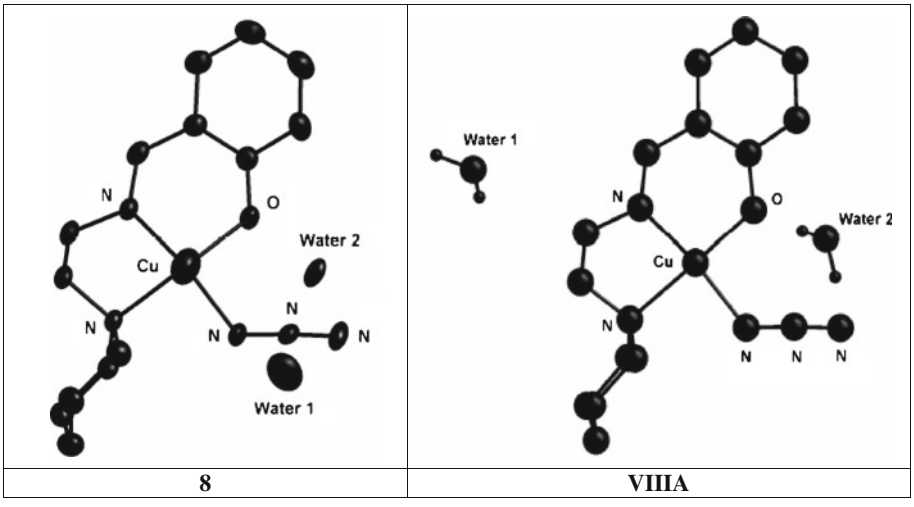

8 **VIIIA**

Figure 14. Perspective views in almost same orientation of $[Cu^{II}L^5(\mu_{1,3}\text{-}N_3)]_n{\cdot}2nH_2O$ (**8**) and $[Cu^{II}L^5(\mu_{1,3}\text{-}N_3)]_n{\cdot}2nH_2O$ (**VIIIA**) demonstrating the difference in location of the two solvated water molecule in the two structures.[28,34,35]

two-dimensional (figure S12). Thus, **8** and **VIIIA** also represent rare example of supramolecular isomerism.

6. Conclusions

The outcome of the research work reviewed here can be summarized as follows: (i) unique observation of a pair of compounds for which all but one parameters, governing magnetic exchange interaction, are identical; (ii) unique example of bridge distance dependency of exchange integral; (iii) rare determination of several density functional theoretical magneto-structural correlations in heterobridged systems; (iv) profound role of asymmetry in the two nickel–azide bond distances in governing the exchange integral in heterobridged μ-phenoxo-$\mu_{1,1}$-azide dinickel(II) systems, as obtained both experimentally and theoretically; (v) unique examples of only single end-to-end azide bridged tetranuclear complexes; (vi) observation of unprecedented small value, 3.3°, of Ni–N···N–Ni torsion angle; (vii) demonstration of overall antiferromagnetic interaction in one single end-to-end azide bridged Ni^{II}_4 system and overall ferromagnetic interaction in the second similar system as the function of the Ni–N···N–Ni torsion angles; (viii) reasonable/excellent matching of the DFT-computed and experimental J values; (ix) nice matching of the trends of the experimental $\chi_M T$ data with the $\chi_M T$ data obtained from the DFT-computed J values; (x) first example of a ferromagnetically coupled end-to-end cyanate bridged one-dimensional copper(II) system; (xi) a unique pair representing new type of magnetic isomerism, new type of crystallographic isomerism and rare type of supramolecular isomerism.

Supplementary material

Figures S1–S12 and table S1 are available at http://www.ias.ac.in/chemsci.

Acknowledgements

Financial support from Government of India through the Department of Science and Technology (DST) (Project to SM) and the University Grants Commission (Fellowship to SS) are gratefully acknowledged.

References

1. (a) Kahn O 1993 In *Molecular magnetism*; New York: VCH; (b) Willet R D, Gatteschi D, Kahn O (eds) 1985 *Magneto-structural correlations in exchange coupled systems*; Dordrecht, The Netherlands: Reidel; (c) O'Connor C J (ed.) 1993 *Research frontiers in magnetochemistry*; World Scientific: Singapore; (d) Ribas J, Escuer A, Monfort M, Vicent R, Cortés R, Lezam L and Rojo T 1999 *Coord. Chem. Rev.* **193** 1027
2. (a) Thompson L K, Mandal S K, Tandon S S, Bridson J N and Park M K 1996 *Inorg. Chem.* **35** 3117; (b) Nanda K K, Thompson L K, Bridson J N and Nag K 1994 *Chem. Commun.* 1337; (c) Mohanta S, Nanda K K, Thompson L K, Flörke U and Nag K 1998 *Inorg. Chem.* **37** 1465; (d) Chaudhuri P, Wagner R, Khanra S and Weyhermuller T 2006 *Dalton Trans.* 4962
3. (a) Palacios M A, Mota A J, Perea-Buceta J E, White F J, Brechin E K and Colacio E 2010 *Inorg. Chem.* **49** 10156; (b) Halcrow M A, Sun J S, Huffman J C and Christou G 1995 *Inorg. Chem.* **34** 4167
4. (a) Ruiz E, Cano J, Alvarez S and Alemany P 1998 *J. Am. Chem. Soc.* **120** 11122; (b) Ruiz E, Alemany P, Alvarez S and Cano J 1997 *J. Am. Chem. Soc.* **119** 1297; (c) Cauchy T, Ruiz E and Alvarez S 2006 *J. Am. Chem. Soc.* **128** 15722; (d) Manca G, Cano J and Ruiz E 2009 *Inorg. Chem.* **48** 3139; (e) Triki S, Gómez-García C J, Ruiz E and Sala-Pala J 2005 *Inorg. Chem.* **45** 5501
5. (a) Winpenny R, (ed) 2006 *Single-molecule magnets and related phenomena*; Springer: New York; (b) Miller J S, Drillon M, (eds) 2001 *Magnetism: Molecules to materials II*; Willey-VCH: Weinheim
6. (a) Beer P D and Gale P A 2001 *Angew. Chem. Int. Ed.* **40** 486; (b) Lehn J-M 1995 In *Supramolecular chemistry*; Weinheim: VCH, (c) Robson R 2000 *Dalton Trans.* 3735; (d) Sauvage J-P, Ed. 1999 *Transition metals in supramolecular chemistry*; *Perspectives in supramolecular chemistry*, London: Wiley, Vol. 5; (e) Blake A J, Champness N R, Hubberstey P, Withersby M A and Schröder M 1999 *Coord. Chem. Rev.* **183** 117; (f) Lin H-H, Mohanta S, Lee C-J and Wei H-H 2003 *Inorg. Chem.* **42** 1584; (g) Nayak M, Koner R, Lin H-H, Flörke U, Wei H-H and Mohanta S 2006 *Inorg. Chem.* **45** 10764; (h) Hazra S, Koner R, Nayak M, Sparkes H A, Howard J A K and Mohanta S 2009 *Cryst. Growth Des.* **9** 3603; (i) Nayak M, Jana A, Fleck M, Hazra S and Mohanta S 2010 *Cryst. Eng. Commun.* **12** 1416; (j) Sasmal S, Majumder S, Hazra S, Sparkes H A, Howard J A K, Nayak M and Mohanta S 2010 *Cryst. Eng. Commun.* **12** 4131
7. Awaga K, Suzuki Y, Hachisuka H and Takeda K 2006 *J. Mater. Chem.* **26** 2516
8. (a) Ring D J, Aragoni M C, Champness N R and Wilson C 2005 *Cryst. Eng. Commun.* **7** 621; (b) Zhang J-P and Kitagawa S 2008 *J. Am. Chem. Soc.* **130** 907
9. Poulsen R D, Overgaard J, Schulman A, Østergaard C, Murillo C A, Spackman M A and Iversen B B 2009 *J. Am. Chem. Soc.* **131** 7580
10. Ma L and Lin W 2008 *J. Am. Chem. Soc.* **130** 13834
11. (a) Feng P L, Stephenson C J, Amjad A, Ogawa G, Barco E d and Hendrickson D N 2010 *Inorg. Chem.* **49** 1304; (b) Clemente-Juan J M, Mackiewicz C, Verelst M, Dahan F, Bousseksou A, Sanakis Y and Tuchagues J-P 2002 *Inorg. Chem.* **41** 1478
12. Demeshko S, Leibeling G, Dechert S and Meyer F 2006 *Dalton Trans.* 3458
13. Milios C J, Prescimone A, Sanchez-Benitez J, Parsons S, Murrie M and Brechin E K 2006 *Inorg. Chem.* **45** 7053

14. Demeshko S, Leibeling G, Maringgele W, Meyer F, Mennerich C, Klauss H-H and Pritzkow H 2005 *Inorg. Chem.* **44** 519
15. Liu G-F, Ren Z-G, Li H-X, Chen Y, Li Q-H, Zhang Y and Lang J-P 2007 *Eur. J. Inorg. Chem.* 5511
16. Zhang Y-Z, Wernsdorfer W, Pan F, Wang Z-M and Gao S 2006 *Chem. Commun.* 3302
17. Gu Z-G, Song Y, Zuo J-L and You X-Z 2007 *Inorg. Chem.* **46** 9522
18. (a) Hong C S, Koo J-E, Son S-K, Lee Y S, Kim Y-S and Do Y 2001 *Chem.–Eur. J.* **7** 4243; (b) Vicente R, Escuer A, Peñalba E, Solans X and Font-Bardía M 1994 *J. Chem. Soc., Dalton Trans.* 3005
19. (a) Goher M A S, Escuer A, Mautne F A and Al-Salem N A 2002 *Polyhedron* **21** 1871; (b) Escuer A,Vicente R, Ribas J, Fallah M S E and Solans X 1993 *Inorg. Chem.* **32** 1033; (c) Liu X-T, Wang X-Y, Zhang W-X, Cui P and Gao S 2006 *Adv. Mater.* **18** 2852; (d) Monfort M, Resino I, Ribas J, Solans X, Font-Bardía M and Stoeckli-Evans H 2002 *New J. Chem.* **26** 1601
20. Stamatatos T C, Abboud K A, Wernsdorfer W and Christou G 2006 *Angew. Chem. Int. Ed.* **45** 4134
21. (a) Bell A, Aromí G, Teat S J, Wernsdorfer W and Winpenny R E P 2005 *Chem. Commun.* 2808; (b) Luo J, Zhou X-G, Weng L-H and Hou X-F 2003 *Acta Crystallogr., Sec. C*: *Cryst. Struct. Commun.* **59** m519
22. (a) Papaefstathiou G S, Perlepes S P, Escuer A, Vicente R, Font-Bardía M and Solans X 2001 *Angew.Chem., Int. Ed.* **40** 884; (b) Boudalis A K, Sanakis Y, Clemente–Juan J M, Donnadieu B, Nastopoulos V, Mari A, Coppel Y, Tuchagues J-P and Perlepes S P 2008 *Chem.–Eur. J.* **14** 2514
23. Meyer F, Kircher P and Pritzkow H 2003 *Chem. Commun.* 774
24. Koner R, Hazra S, Fleck M, Jana A, Lucas C R and Mohanta S 2009 *Eur. J. Inorg. Chem.* 4982
25. Hazra S, Koner R, Lemoine P, Sañudo E C and Mohanta S 2009 *Eur. J. Inorg. Chem.* 3458
26. Sasmal S, Hazra S, Kundu P, Dutta S, Rajaraman G, Sañudo E C and Mohanta S 2011 *Inorg. Chem.* **50** 7257
27. Sasmal S, Hazra S, Kundu P, Majumder S, Aliaga-Alcalde N, Ruiz E, Mohanta S 2010 *Inorg. Chem.* **49** 9517
28. Sasmal S, Sarkar S, Aliaga-Alcalde N and Mohanta S 2011 *Inorg. Chem.* **50** 5687
29. Figures 1 and 3 in this article are redrawn in comparison to the figures 1 and 3 in ref. 24. Copyright Wiley-VCH Verlag GmbH & Co. KGaA. Reproduced with permission.
30. Figures 2 and 7 in this article are redrawn in comparison to the figures 1 and 12 in ref. 26. Figures 4, 5 and 6 and table 1 in this article are adapted after slight redrawing/modification of the figures 3, 10 and 11 and table 3 in ref. 26. Copyright American Chemical Society. Reprinted (adapted) with permission.
31. (a) Dey S K, Mondal N, Fallah M S E, Vicente R, Escuer A, Solans X, Font-Bardía M, Matsushita T, Gramlich V and Mitra S 2004 *Inorg. Chem.* **43** 2427; (b) Banerjee A, Singh R, Chopra D, Colacio E and Rajak K K 2008 *Dalton Trans.* 6539
32. The Noodleman's BS approach; B3LYP exchange–correlation functional; valence triple-zeta quality basis sets (TZV) of Ahlrichs and coworkers; GAUSSIAN 03 suite of programs with an initial guess made using Jaguar 7.0
33. Figures 8 and 9 in this article are redrawn in comparison to the figures 1 and 2 in ref. 27. Figures 10 and 11 in this article are adapted after slight redrawing/modification of the figures 3 and 4 in ref. 27. Copyright American Chemical Society. Reprinted (adapted) with permission.
34. Mukherjee P S, Dalai S, Mostafa G, Lu T-H, Rentschler E and Chaudhuri N R 2001 *New J. Chem.* **25** 1203
35. A part of figure 12 (for compound 8) and figure 14 in this article are redrawn in comparison to the figures 2 and S9 in ref. 28. Figure 13 in this article is adapted after slight redrawing/modification of the figure 4 in ref. 28. Copyright American Chemical Society. Reprinted (adapted) with permission. Another part of figure 12 (for compound VIIIA) is drawn taking CIF from the Cambridge Structural Database (Version 5.32, 2011), the Cambridge Crystallographic Data Centre.
36. B3LYP exchange–correlation functional; basis set of triple-ζ quality as proposed by Schaefer *et al*; Gaussian09 code using guess functions generated with the Jaguar 7.0 code
37. Baker G A, Rushbrooke G S and Guilbert H E 1964 *Phys. Rev.* **135** A1272